JOURNAL OF MATERIALS SCIENCE 32 (1997) 5163–5167

Texture control and the anisotropy of mechanical properties in titanium sheet

Z. S. ZHU, R. Y. LIU, M. G. YAN, C. X. CAO
Beijing Institute of Aeronautical Materials, Beijing 100095, People's Republic of China
J. L. GU, N. P. CHEN
Department of Materials Science and Engineering, Tsinghua University, Beijing 100084, People's Republic of China

By means of three-dimensional crystallite orientation distribution function (CODF) analysis, the relationship between texture control processes and mechanical properties anisotropy in titanium sheet has been investigated. The formation and transition of cold-rolling texture, recrystallization texture and phase transformation texture are also discussed. The results show that, after being cold rolled unidirectionally and annealed, titanium sheet exhibits a strong anisotropy of mechanical properties due to the pyramidal textures $(\bar{2}\,1\,1\,5)$ $[0\,\bar{1}\,1\,0]$ and $(\bar{1}\,0\,1\,3)$ $[1\,\bar{2}\,1\,0]$. After a cyclic phase transformation process coupled with cold rolling and annealing treatment, the recrystallization texture component $(\bar{1}\,0\,1\,3)$ $[1\,\bar{2}\,1\,0]$ is suppressed and $[h\,k\,i\,l] \parallel$ ND transformation fibre texture (where ND is the sheet normal direction) are developed, which produce a well improved mechanical anisotropy. The cross-rolling process can create a basal type texture $(0\,0\,0\,2)$ $\langle u\,v\,t\,w\rangle$ or a near basal type texture, which leads to low level planar mechanical properties anisotropy but to relatively high normal plastic anisotropy (R value)

1. Introduction

The very pronounced textures in rolled titanium sheets give rise to strong mechanical properties anisotropy [1], and have a detrimental influence on the other properties, such as fatigue, creep [2], working and shaping behaviours [3]. While developing an ideal $(0\,0\,0\,2)\langle u\,v\,t\,w\rangle$ texture (basal type texture) in hexagonal close packed (hcp) metal titanium, a significant strength advantage under biaxial stress can be achieved. This biaxial strengthening has been termed "texture hardening" by Backofen and is related to the normal anisotropy parameter, R value [4]. So, texture control has become more and more important in recent years, especially for titanium and its alloy owing to their inherent anisotropy and the limited quantity of slip systems. Great efforts in the past have been concentrated on developing a random texture to minimize the anisotropy effects: however, it is now well recognized that significant improvement in mechanical performance can be achieved through texture control. Opportunities for realizing such benefits are particularly attractive for the hcp metals because of their restricted slip behaviour [5].

In the present work, the influence of cold rolling (CR), cold cross-rolling (CCR), hot cross-rolling (HCR) and cyclic phase transformation (CPT) processes on texture formation and mechanical properties anisotropy in titanium sheet is studied by CODF analysis. The mechanism of texture formation in titanium sheet will also be discussed.

2. Experimental procedure

The as-received material was commercially pure titanium plate, containing (in wt %) 0.13 O, 0.11 Fe, 0.02 C, 0.002 H, 0.02 N and < 0.04 Si. The material was cold rolled unidirectionally up to 86% reduction in thickness in eight passes to a final thickness of 1.1 mm and then annealed at 700 °C for 1 h. This process is called the CR process in this paper. The $\alpha \rightarrow \beta \rightarrow \alpha$ phase transformation treatment was realized by heating the cold rolled material at 950 °C (about 50 °C above the $\alpha \rightarrow \beta$ polymorphous transformation temperature) and subsequently being air-cooled. This process was repeated for three cycles, and then the specimens were cold rolled by 20% reduction and annealed at 700 °C for 1 h. This process may be termed the CPT process.

In comparison to the effects of the CR and CPT processes, cross-rolling processes were also applied to the titanium sheet. CCR treatment was realized by rolling the titanium sheet along the direction normal to the original hot-rolling direction at room temperature up to 80% in eight passes to a final thickness of 1.6 mm. The hot cross-rolling procedure (HCR) was performed at 850 °C to a thickness of 8 mm and then cold rolled 30% to a final thickness of 1.2 mm with internal annealing at 760 °C for 1 h. All these final specimens were annealed at 700 °C for 1 h and cooled in air.

The development and transition of textures were investigated by means of CODF analysis that was

calculated through four pole figures (0 0 0 2), $\{1\,0\,\bar{1}\,0\}$, $\{1\,0\,\bar{1}\,1\}$ and $\{1\,0\,\bar{1}\,2\}$ at the mid-thickness of all the specimens, according to the principle of spherical harmonic analysis described by Roe [6] and Liang *et al.* [7]. Contoured plots of CODF were produced for constant ϕ sections in the volume of Euler space $0 \leqslant \psi \leqslant \pi/2$, $0 \leqslant \theta \leqslant \pi/2$ and $0 \leqslant \phi \leqslant \pi/3$. Because the main orientations in hcp titanium are located on $\phi = 0$ and 30° sections of CODF, these two sections of CODF are expressed in this paper.

The yield stress and R values were measured with specimens taken at angles of 0, 45 and 90° from the rolling direction (RD) according to the ASTM testing standard E8-87a. The R value was determined at 5% tensile strain.

3. Results

3.1. Texture analyses

Fig. 1 shows the constant ϕ sections of CODF observed in specimens after being cold rolled to 86% and then annealed at 700 °C for 1 h. From Fig. 1a, it can be seen that, in the specimen cold rolled 86% and annealed, there are two main texture components, i.e. the cold-rolling texture component $(\bar{2}\,1\,1\,5)[0\,\bar{1}\,1\,0]$ and the recrystallization texture component $(\bar{1}\,0\,1\,3)[1\,\bar{2}\,1\,0]$ (Fig. 1b). It is well known that $(\bar{1}\,0\,1\,3)[1\,\bar{2}\,1\,0]$ is developed at the expense of the cold-rolling texture, such as $(\bar{2}\,1\,1\,5)[0\,\bar{1}\,1\,0]$. And these two components are related by a rotation of 30° about the common [0 0 0 1] axis.

Fig. 2a shows the $\phi = 0$ and 30° sections of CODF observed in titanium sheet after three cycles of phase transformation procedure. It can be seen that the texture mainly consists of three types of orientations, i.e. $[\bar{2}\,1\,1\,0] \parallel$ ND fibre texture, $[\bar{2}\,1\,1\,5] \parallel$ ND partial fibre texture and basal components, such as $(0\,0\,0\,2)[3\,\bar{2}\,1\,0]$ (Fig. 2). It should be noted that, after three cycles of $\alpha \rightarrow \beta \rightarrow \alpha$ phase transformation, the original rolling texture component $(\bar{2}\,1\,1\,5)[0\,\bar{1}\,1\,0]$ is transformed into components $(\bar{2}\,1\,1\,5)[5\,\bar{4}\,1\,3]$, $(\bar{2}\,1\,1\,5)[0\,\bar{1}\,1\,0]$ and $(\bar{2}\,1\,1\,5)[5\,\bar{9}\,4\,3]$, etc., distributed along the $\theta = 34°$ line on $\phi = 30°$ section of CODF, tending to form a $[\bar{2}\,1\,1\,5] \parallel$ ND partial fibre texture. And the recrystallization texture component $(\bar{1}\,0\,1\,3)[1\,\bar{2}\,1\,0]$, observed in Fig. 1b after CR treatment, is completely suppressed after the $\alpha \rightarrow \beta \rightarrow \alpha$ phase transformation procedure.

Fig 2b shows the $\phi = 0$ and 30° sections of CODF observed in titanium sheet after the CPT process. The orientation distribution feature is very similar to Fig. 2a. However, the basal orientations, such as $(0\,0\,0\,2)[3\,\bar{2}\,1\,0]$, disappear, and the $[\bar{2}\,1\,1\,5] \parallel$ ND fibre texture observed in Fig. 2a is substituted by a $[\bar{2}\,1\,1\,7] \parallel$ ND partial fibre texture lying along the $\theta = 25°$ line on the $\phi = 30°$ section of CODF.

Figs 3 and 4 show the orientation distributions along the $\theta = 90$ and 25° lines on the $\phi = 30°$ section of CODF observed in specimens after CR and CPT treatment, respectively. It can be seen that, the main texture in the titanium sheet after the CR process consists of isolated orientation peaks $(\bar{2}\,1\,1\,5)[0\,\bar{1}\,1\,0]$ and $(\bar{1}\,0\,1\,3)[1\,\bar{2}\,1\,0]$, but after CPT treatment the texture is characterized by $[\bar{2}\,1\,1\,0] \parallel$ ND and $[\bar{2}\,1\,1\,7] \parallel$ ND fibre textures.

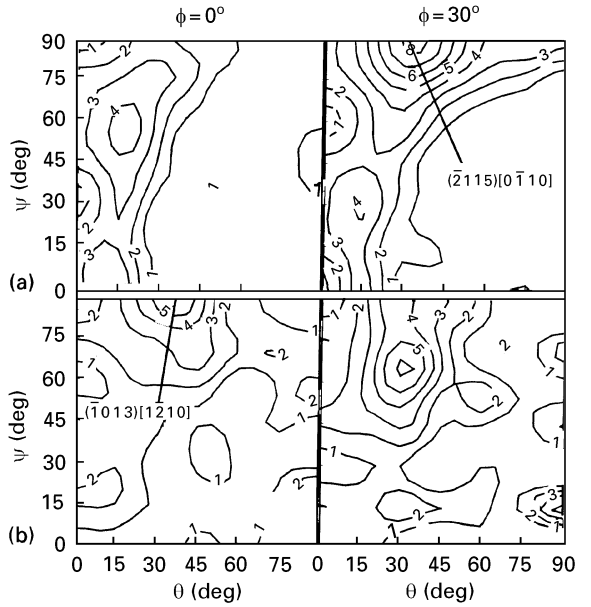

Figure 1 The $\phi = 0$ and 30° sections of CODF observed in specimens (a) as-cold rolled 80% and (b) cold rolled 86% and then annealed at 700 °C for 1 h (CR treatment).

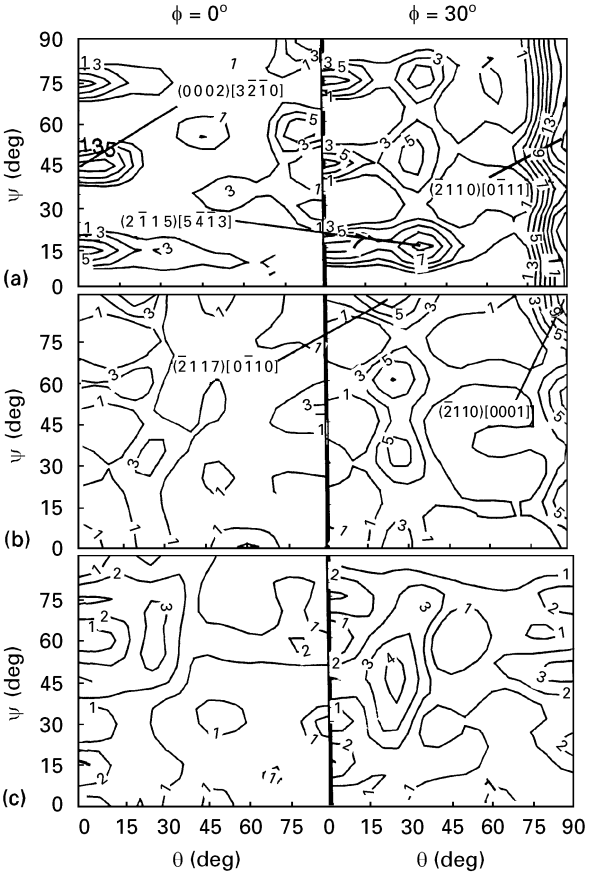

Figure 2 $\phi = 0$ and 30° sections of CODF observed in titanium sheets cold rolled 86%, and conducted by (a) three cycles of $\alpha \rightarrow \beta \rightarrow \alpha$ phase transformation and subsequently followed by rolling (b) 20% (CPT) and (c) 50% , respectively, and annealing at 700 °C for 1 h.

The orientation distribution features observed in specimens after cross-rolling treatment are very different from those observed in specimens after CR and

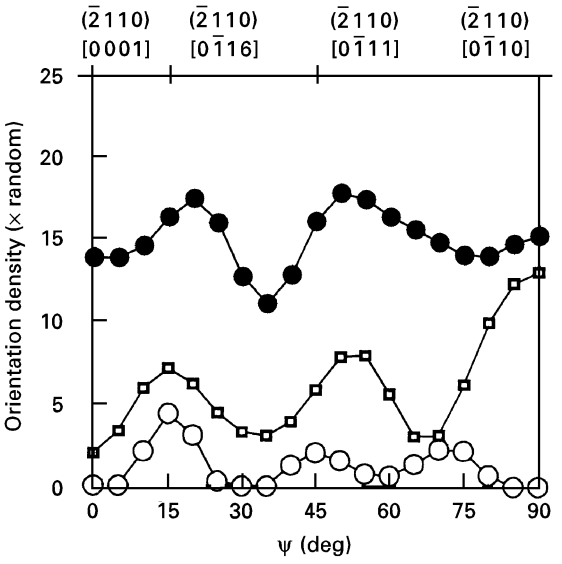

Figure 3 The orientation distributions along the $\theta = 90^\circ$ axis on the $\phi = 30^\circ$ section of CODF observed in specimens after suffering CR (○) three cycles of $\alpha \rightarrow \beta \rightarrow \alpha$ phase transformation (●) and CPT treatment (□), respectively.

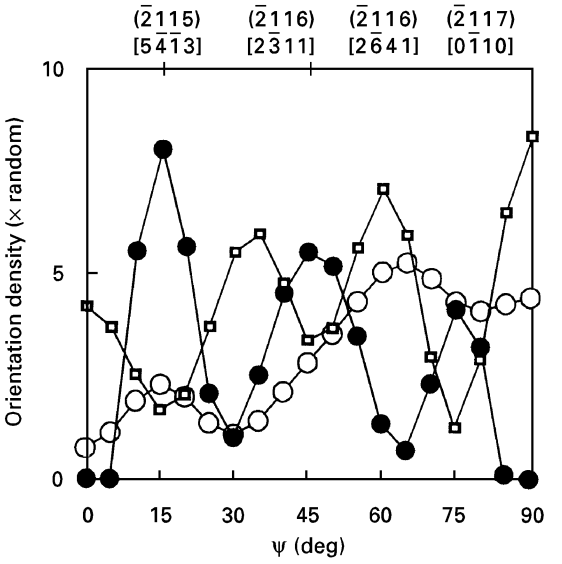

Figure 4 The orientation distributions along the $\theta = 25^\circ$ lines on the $\phi = 30^\circ$ section of CODF observed in specimens after CR (○) three cycles of $\alpha \rightarrow \beta \rightarrow \alpha$ phase transformation (●) and CPT treatment (□), respectively.

CPT treatments. Fig. 5 shows the $\phi = 0$ and 30° sections of titanium sheet after CCR and HCR treatment. It can be seen from Fig. 5a that there are two main fibre textures, $[\bar{2}\,1\,1\,15] \parallel$ ND and $[\bar{2}\,0\,2\,15] \parallel$ ND, located on the $\phi = 15$–20° lines, deviated but near the $(0\,0\,0\,2)\ \langle u\,v\,t\,w\rangle$ basal type texture.

Fig 5b shows the orientations observed in specimens after HCR treatment. The main texture is composed of $(0\,0\,0\,2)\langle 1\bar{4}\,3\,0\rangle$ basal type texture components, with the orientations more randomly distributed with a relatively low density.

3.2. Mechanical properties anisotropy

Fig. 6 shows the anisotropies of the 0.2% proof yield stress, $\sigma_{0.2}$ and the normal anisotropy parameter

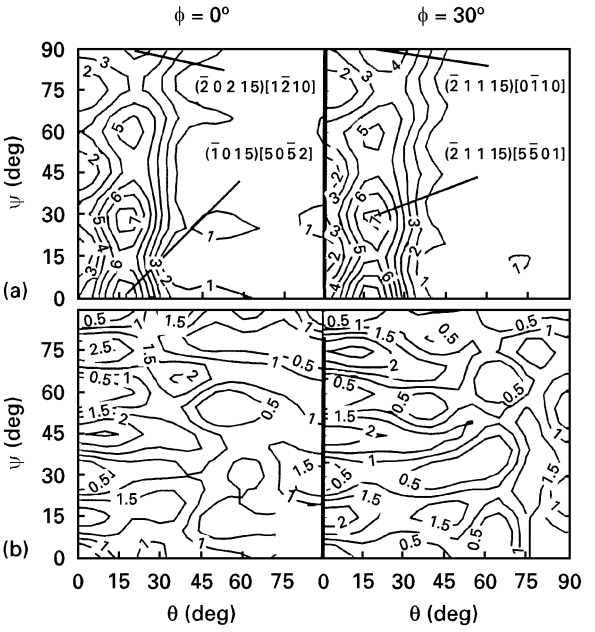

Figure 5 The $\phi = 0$ and 30° sections of CODF observed in specimens after (a) CCR and (b) HCR treatment, respectively.

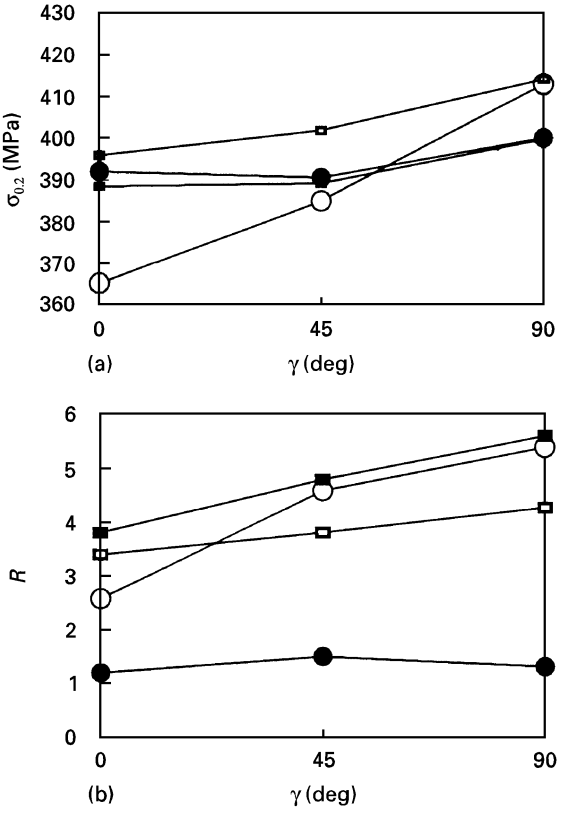

Figure 6 The yield stress (0.2% proof stress) (a) and R value (b) with the angle γ from the rolling direction of titanium sheets conducted by (○) CR, (●) CPT, (□) CCR and (■) HCR, respectively.

R value observed in titanium sheet after different treatment processes. It is indicated that, the yield stress anisotropy of titanium sheet after the CR process is quite large, with the difference between TD and RD as large as 50 MPa. However, in specimens after CPT treatment, the anisotropy of the yield stress is highly minimized. The anisotropy trend of the R values is very similar to that of the yield stress. But

the R value of the titanium sheet is lowest after CPT and highest after HCR (see Fig. 6).

All these features can be explained well by the deformation behaviour and the texture orientation distribution in the titanium sheets.

4. Discussion

4.1. Mechanical properties anisotropy

It is well known that textures can induce pronounced anisotropies in mechanical properties, especially for hcp metals like α-titanium because of its restricted slip behaviour [8].

From Fig. 6 it can be seen that, in cold rolled and annealed (CR process) titanium sheet, pronounced anisotropies of yield stress and R value are produced. These phenomena may probably be associated with the development of texture components $(\bar{2}\,1\,1\,5)[0\,\bar{1}\,1\,0]$ and $(\bar{1}\,0\,1\,3)[1\,\bar{2}\,1\,0]$ in titanium sheet after CR treatment. Because the textures $(\bar{2}\,1\,1\,5)[0\,\bar{1}\,1\,0]$ and $(\bar{1}\,0\,1\,3)[1\,\bar{2}\,1\,0]$ are related by a rotation of 30° about the [0 0 0 2] direction, and make the c-axis inclined about 32° from ND to TD, the active deformation mechanism will be different while the tensile axis is along RD or TD. It can be deduced that, when the tensile stress axis is along RD, deformation must be accommodated by the operation of the more easy $\{1\,\bar{1}\,0\,0\}\langle 1\,1\,\bar{2}\,0\rangle$ prismatic slip mode. On the other hand, when the tensile stress axis is along TD, the deformation mode will be the more difficult $(0\,0\,0\,2)\langle 1\,\bar{2}\,1\,0\rangle$ basal slip or $\langle c+a\rangle$ slip, because the critical resolved shear stress for basal slip $(0\,0\,0\,2)\langle 1\,\bar{2}\,1\,0\rangle$ is about four times that for prismatic slip $\{1\,\bar{1}\,0\,0\}\langle 1\,1\,\bar{2}\,0\rangle$ at room temperature [9]. This is the reason why the cold rolling and recrystallization pyramidal textures $(\bar{2}\,1\,1\,5)[0\,\bar{1}\,1\,0]$ and $(\bar{1}\,0\,1\,3)[1\,\bar{2}\,1\,0]$ can induce a pronounced mechanical properties anisotropy.

However, the $(0\,0\,0\,2)\langle u\,v\,t\,w\rangle$ basal type texture and $[h\,k\,i\,l]\parallel$ ND fibre texture can activate the deformation mechanisms in relatively equal probability when tensile stress is applied along RD or TD, which results in planar isotropic mechanical properties.

4.2. Texture control

Texture control can provide beneficial use of the variety of textures available in hcp titanium alloys. A classic example is the improved deep drawing performance achieved through texture control that provides high thinning resistance and a low level of planar anisotropy [10].

Therefore, the aim of texture control is to suppress the pyramidal texture components, such as $(\bar{2}\,1\,1\,5)[0\,\bar{1}\,1\,0]$ and $(\bar{1}\,0\,1\,3)[1\,\bar{2}\,1\,0]$, through certain texture control processes by forming the ideal $(0\,0\,0\,1)\langle u\,v\,t\,w\rangle$ basal type texture and the $[h\,k\,i\,l]\parallel$ ND fibre texture. The former, e.g. basal type texture $(0\,0\,0\,2)\langle u\,v\,t\,w\rangle$ or a deviating but near basal type texture, can be created through CCR and HCR processes shown in Fig. 5 to provide a high degree of normal anisotropy (R value) and a low level of planar anisotropy of yield stress (Fig. 6). The latter $[h\,k\,i\,l]\parallel$ ND fibre texture can be realized through the CPT process, which can also provide the lowest planar anisotropy of yield stress and R values (Fig. 6).

Nevertheless, the cross-rolling procedure requires repeated changes in rolling direction, which restricts the geometric dimensions of the initial and final product sheets, and consequently increases the product cost and labour strength. So the cross-rolling process cannot be used extensively in practical production. From a fabricability standpoint, the CPT process will be the most effective in texture control processes.

4.3. The formation mechanism of the $[h\,k\,i\,l]\parallel$ND fibre texture during the CPT process in titanium sheet

When a phase transformation takes place in titanium, there is a definite orientation relationship between parent and product phases, namely, the Burger's relationship, i.e. $\{1\,1\,0\}_\beta\parallel(0\,0\,0\,1)_\alpha$, $\langle 1\,\bar{1}\,1\rangle_\beta\parallel\langle 1\,1\,\bar{2}\,0\rangle_\alpha$ [11]. As a result, the transformed phase will acquire a correspondent texture due to the parent phase texture after a phase transformation occurs [12]. According to the Burger's relationship, the rolling texture component $(\bar{2}\,1\,1\,5)[0\,\bar{1}\,1\,0]$ and the recrystallization texture component $(\bar{1}\,0\,1\,3)[1\,\bar{2}\,1\,0]$ may probably transform to $\{1\,1\,3\}\langle 1\,2\,\bar{1}\rangle$, $\{1\,1\,4\}\langle 1\,3\,\bar{1}\rangle$, $\{0\,0\,1\}\langle 1\,0\,0\rangle$, $\{1\,1\,2\}\langle 1\,1\,\bar{1}\rangle$ and $\{1\,1\,1\}\langle 1\,1\,0\rangle$, etc. after an $\alpha\rightarrow\beta$ transformation. Because the orientations $\{1\,1\,3\}\langle 1\,2\,\bar{1}\rangle$ and $\{0\,0\,1\}\langle 1\,0\,0\rangle$ are related by a rotation angle of about 25° about their common axis $\langle 1\,1\,1\rangle$, the grains with $\{0\,0\,1\}\langle 1\,0\,0\rangle$ orientation may preferentially develop at the expense of the grains with the orientation $\{1\,1\,3\}\langle 1\,2\,\bar{1}\rangle$ during the hold time at the β phase temperature. By using a high temperature X-ray diffraction technique (HTXRD), it is found that the main orientations of the β phase at 950 °C are $\{0\,0\,1\}$ planes that are parallel to the sheet rolling plane [13, 14]. So the main orientations in the β phase consist of $\{0\,0\,1\}\langle 1\,0\,0\rangle$, $\{0\,0\,1\}\langle 1\,\bar{1}\,0\rangle$, $\{1\,1\,1\}\langle 1\,\bar{1}\,0\rangle$ and $\{1\,1\,2\}\langle 1\,1\,\bar{1}\rangle$ after cold rolled titanium sheet after an $\alpha\rightarrow\beta$ phase transformation.

Similarly, according to Burger's relationship, starting with a single component of β phase, a total of 12 reorientations may arise with equal probability after $\beta\rightarrow\alpha$ phase transformation. In fact, there exists orientation variant selection during $\beta\rightarrow\alpha$ phase transformation that results in the formation of $[\bar{2}\,1\,1\,0]\parallel$ ND fibre texture, with the cold-rolling texture $(\bar{2}\,1\,1\,5)[0\,\bar{1}\,1\,0]$ and recrystallization texture $(\bar{1}\,0\,1\,3)[1\,\bar{2}\,1\,0]$ being suppressed [13].

At the same time, the reappearance of original rolling texture components, such as $(\bar{2}\,1\,1\,5)[0\,\bar{1}\,1\,0]$, $(\bar{2}\,1\,1\,5)[5\,\bar{4}\,1\,3]$ and $(\bar{2}\,1\,1\,5)[5\,\bar{9}\,4\,3]$, forming a $[\bar{2}\,1\,1\,5]\parallel$ ND partial fibre texture, can be explained by the reversion of the orientations $\{1\,1\,1\}\langle 1\,1\,0\rangle$ and $\{1\,1\,2\}\langle 1\,1\,1\rangle$ after $\beta\rightarrow\alpha$ phase transformation. So these facts imply that the formation of the transformation texture $[\bar{2}\,1\,1\,0]\parallel$ ND and texture $[\bar{2}\,1\,1\,0]\parallel$ ND satisfy Burger's relationship of existing orientation variant selection. The mechanism of orientation variant selection has been described in detail in previous work [15].

However, the (0002) basal type textures formed after three cycles of $\alpha \rightarrow \beta \rightarrow \alpha$ phase transformation cannot be explained directly through Burger's relationship. Because if basal (0002) orientations are formed through Burger's relationship, a parent orientation in the β phase will probably be $\{0\,1\,1\}\langle 0\,0\,1\rangle$, but which can be found neither by HTXRD analysis nor by calculation through Burger's relationship. However, the orientations $\{1\,1\,1\}\langle 1\,1\,2\rangle$ and $\{1\,1\,0\}\langle 0\,0\,1\rangle$ in the β phase are related by 35° about their common axis $\langle 1\,1\,0\rangle$. So it is possible that, after three cycles of $\alpha \rightarrow \beta \rightarrow \alpha$ phase transformation, the orientations $\{1\,1\,0\}\langle 0\,0\,1\rangle$ will be preferentially developed at the expense of orientations $\{1\,1\,1\}\langle 1\,1\,2\rangle$. For detailed discussion refer to [16].

5. Conclusions

1. After being rolled and annealed, titanium sheet exhibits a pronounced mechanical properties anisotropy due to the pyramidal texture components $(\bar{2}\,1\,1\,5)[0\,\bar{1}\,1\,0]$ and $(\bar{1}\,0\,1\,3)[1\,\bar{2}\,1\,0]$.

2. The suppression of pyramidal texture components and formation of a more beneficial texture orientation distribution are possible through some texture control processes. The developments of the $(0\,0\,0\,2)\langle u\,v\,t\,w\rangle$ basal type texture and the $[h\,k\,i\,l] \parallel \mathrm{ND}$ fibre texture are the two more effective approaches in this paper.

3. Cross-rolling processes can provide a basal type texture or a deviated but near basal type texture, which can produce a high degree of normal anisotropy (R value) and a low level of planar anisotropy of yield stress.

4. The process of $\alpha \rightarrow \beta \rightarrow \alpha$ phase transformation, coupled with cold rolling and annealing treatment, is proved to be the most effective texture control process, by which the $[\bar{2}\,1\,1\,0] \parallel \mathrm{ND}$ and $[\bar{2}\,1\,1\,7] \parallel \mathrm{ND}$ fibre textures are formed and the isotropic planar mechanical properties are achieved.

5. The suppression of pyramidal textures and the formation of fibre textures satisfy Burger's relationship, but orientation variant selection must be taken into account in this case.

Acknowledgements

The authors are grateful to the National Education Committee of the People's Republic of China for the financial support of the Doctoral Foundation, and the Central Iron and Steel Research Institute, Beijing, China for some experimental facilities. The experimental material was provided by Baoji Nonferrous Metals Works, People's Republic of China.

References

1. H. INAGAKI, *Z. Metallkd.* **83** (1992) 40.
2. H. PUSCHNIK, J. FLADISCHER, G. LUTJERING and R. S. JAFFEE, in "*Ti'92*: *science and technology*", edited by F. H. Froes and I. Caplan (The Minerals, Metals & Materials Society, TMS, Warrendale, PA, USA 1993) p. 131.
3. E. H. RENNHACK and D. D. CROOKS, *Metall. Trans. A* **10A** (1979) 457.
4. W. F. HOSFORD, *Met. Eng. Qty.* **6** (1966) 13.
5. K. L. MURTY, *Metals Forum* **15** (1991) 217.
6. R. J. ROE, *J. Appl. Phys.* **36** (1965) 2024.
7. Z. D. LIANG, J. Z. XU and F. WANG, *Texture Cryst. Solids* **4** (1980) 93.
8. R. M. TCHORZEWSKI and W. B. HUTCHINSON, *Met. Sci.* **2** (1978) 109.
9. E. D. LEVINE, *Trans. AIME* **236** (1966) 1558.
10. A. HASEGAWA, T. NISHIMURA and M. FUKUDA, in "*Titanium and titanium alloys*: *scientific and technological aspects*" (Plenum Press, Moscow, USSR, 1982) p. 1947.
11. R. K. MCEARY and B. LUSTMAN, *Trans. AIME* **191** (1951) 994.
12. G. J. DAVIES, J. S. KALLEND and P. P. MORRIS, *Acta Metall.* **24** (1976) 159.
13. Z. S. ZHU, J. L. GU and N. P. CHEN, *Scripta Metall. Mater.* **32** (1995) 499.
14. *Idem*, *J. Mater. Sci. Lett.* **14** (1995) 1153.
15. Z. S. ZHU, J. L. GU, N. P. CHEN and M. G. YAN, *ibid.* **15** (1996) 76.
16. Z. S. ZHU, J. L. GU and N. P. CHEN, *Acta Metall. Sinica* **2** (1996) in Chinese **32** (1996) 127.

Received 23 February 1996
and accepted 18 February 1997